Comparative Proteome Analysis of Native Differentiated and Cultured Dedifferentiated Human RPE Cells

Claudia S. Alge,[1,2] *Sabine Suppmann,*[2,3] *Siegfried G. Priglinger,*[1] *Aljoscha S. Neubauer,*[1] *Christian A. May,*[4] *Stefanie Hauck,*[2,3] *Ulrich Welge-Lussen,*[1] *Marius Ueffing,*[2,3,5] *and Anselm Kampik*[1,4,5]

Purpose. Dedifferentiation of retinal pigment epithelial (RPE) cells is a crucial event in the pathogenesis of proliferative vitreoretinopathy (PVR). This study was designed to improve the understanding of RPE cell dedifferentiation in vitro. The protein expression pattern of native differentiated RPE cells was compared with that of cultured, thereby dedifferentiated, RPE cells.

Methods. Differentiated native human RPE cells and monolayers of dedifferentiated cultured primary human RPE cells were processed for two-dimensional (2-D) electrophoresis. Total cellular proteins were separated by isoelectric focusing using immobilized pH gradients (IPG 3–10) and electrophoresis on 9% to 15% gradient polyacrylamide gels. Proteins were visualized by silver staining. Silver-stained gel spots were excised, digested in situ, and analyzed by matrix-assisted laser desorption ionization time of flight (MALDI-TOF) mass spectroscopy (MS). The resultant peptide mass fingerprints were searched against the public domain NCBInr, MSDB, and EnsemblC databases to identify the respective proteins.

Results. One hundred seventy nine protein spots were analyzed and classified into functional categories. Proteins associated with highly specialized functions of the RPE, which are required for interaction with photoreceptor cells, including RPE65, cellular retinaldehyde-binding protein (CRALBP), and cellular retinol-binding protein (CRBP), were absent in dedifferentiated cultured RPE cells, whereas proteins involved in phagocytosis and exocytosis, including cathepsin D and clathrin were still present. Dedifferentiated RPE cells displayed a strong shift toward increased expression of proteins associated with cell shape, cell adhesion, and stress fiber formation, including cytokeratin 19, gelsolin, and tropomyosins, and also acquired increased expression of factors involved in translation and tumorigenic signal transduction such as annexin I and translation initiation factor (eIF)-5A.

Conclusions. Dedifferentiation of human RPE cells in vitro results in downregulation of proteins associated with highly specialized functions of the RPE and induces the differential expression of proteins related to cytoskeleton organization, cell shape, cell migration, and mediation of proliferative signal transduction. These in vitro data suggest that the dedifferentiated status of RPE cells per se may initiate PVR. Further investigation of candidate proteins may identify additional targets for treatment or prevention of diseases associated with RPE dedifferentiation. (*Invest Ophthalmol Vis Sci.* 2003;44: 3629–3641) DOI:10.1167/iovs.02-1225

In the adult, the retinal pigment epithelium (RPE) is a mosaic of polygonal, postmitotic cells interposed between the choroid and the neural retina and serves as the outer blood–retinal barrier regulating retinal homeostasis and visual function.[1,2] The apical side of RPE cells closely associates with the outer segments of cones and rods, whereas the base of the cell attaches to Bruch's membrane. Normally RPE cells form a quiescent monolayer, but they retain the ability to divide and do so when placed in culture[2,3] or when participating in wound repair. RPE cells proliferate readily in vivo in response to a variety of stimuli such as photocoagulation and/or retinal cryotherapy.[4,5] In mild injuries, involving only the RPE and photoreceptor cells, proliferating RPE cells quickly reestablish a continuous monolayer.[6,7] However, after severe injury that may be associated with ocular trauma or retinal detachment, RPE cells can be detached and consequently found in the vitreous. Once in this new environment, RPE cells have been shown to dedifferentiate and exhibit a pseudometaplastic transformation into fibroblast-like, spindle-shaped cells, which become actively dividing and migratory.[1,8–11] These processes are considered to be key events in the onset of proliferative vitreoretinopathy (PVR).[12–19]

In an animal model of PVR, Radtke et al.[19] demonstrated that when RPE cells are injected into the vitreous, they cause the formation of contractile vitreal and periretinal membranes. However, this effect is more pronounced when cultured, thus dedifferentiated, RPE cells are injected than when freshly isolated native RPE cells are placed in the vitreous cavity.

Adult human RPE cells in culture escape growth arrest and fail to maintain a differentiated morphology and[20] rapidly dedifferentiate at the molecular level, and markers of RPE differentiation such as RPE65 and RET-PE 10 quickly become undetectable.[21,22] It has also been reported that expression of intermediate filaments is altered when the cells take on fusiform morphology[23,24] and that polarity may be partially lost.[25–27] Thus, dedifferentiated proliferative RPE cell cultures have been used to study the very early phases of PVR, both in vitro and in vivo.[16,19,28–32]

However, the molecular changes associated with dedifferentiation of RPE cells per se are not well understood, and to our knowledge, the overall cellular proteome of native differ-

From the [1]Department of Ophthalmology and the [2]Clinical Cooperation Group Ophthalmogenetics, Ludwig-Maximilians-University, Munich, Germany; the [3]German Research Center of Environment and Health, Oberschleissheim, Germany; and the [4]Department of Anatomy II, University of Erlangen-Nürnberg, Erlangen, Germany.

[5]Contributed equally to the work and therefore should be considered equivalent senior authors.

Supported by the German Federal Ministry for Education and Research Grants FKZ:031U108A (MU), PRORET QLK6-CT-2000-00569 (MU), PRO AGE-RET QLK-CT-2001-00385 (MU); German Research Foundation Grant WE 2577/2-1; and German Ophthalmological Society Research Support (UW-L).

Submitted for publication November 29, 2002; revised February 12, 2003; accepted March 3, 2003.

Disclosure: **C.S. Alge**, None; **S. Suppmann**, None; **S.G. Priglinger**, None; **A.S. Neubauer**, None; **C.A. May**, None; **S. Hauck**, None; **U. Welge-Lussen**, None; **M. Ueffing**, None; **A. Kampik**, None

The publication costs of this article were defrayed in part by page charge payment. This article must therefore be marked "*advertisement*" in accordance with 18 U.S.C. §1734 solely to indicate this fact.

Corresponding author: Anselm Kampik, Department of Ophthalmology, Ludwig-Maximilians-University, Munich, Germany; anselm.kampik@ak-i.med.uni-muenchen.de.

entiated RPE cells has not been characterized to date. The goal of the present study was to gain better understanding of the process of RPE cell dedifferentiation in vitro. We therefore took a proteomic approach to investigate the shift in the overall protein expression pattern between differentiated native human RPE cells and dedifferentiated cultured RPE cells. With this approach we attempted to screen for the most prominent dedifferentiation-related changes in several functional groups simultaneously. The proteomic changes illustrated in this study clearly reflect the dynamic changes in the protein expression pattern associated with dedifferentiation of the RPE. Some of the identified proteins have been described to be associated with RPE dedifferentiation or PVR, whereas other proteins may be newly linked with RPE dedifferentiation and proliferation and have not yet been described in the RPE.

Materials and Methods

Isolation of Human RPE Cells

Eyes from eight human donors were obtained from the Munich University Hospital Eye Bank and processed within 4 to 16 hours after death. The average donor age was 46 ± 6 years. None of the donors had a known history of eye disease. Methods for securing human tissue were humane, included proper consent and approval; complied with the Declaration of Helsinki, and were approved by the local ethics committee. Human retinal pigment epithelium (RPE) cells were harvested according to a procedure described previously.[33] In brief, whole eyes were thoroughly cleansed in 0.9% NaCl solution, immersed in 5% poly(1-vinyl-2-pyrrolidone)-iodine (Jodobac; Bode-Chemie, Hamburg, Germany), and rinsed again in the sodium-chloride solution. The anterior segment from each donor eye was removed, and the posterior poles were examined with the aid of a binocular stereomicroscope to confirm the absence of gross retinal disease. Next, the neural retinas were carefully peeled away from the RPE-choroid-sclera with fine forceps. The eyecup was rinsed with Ca^{2+} and Mg^{2+}-free Hanks' balanced salt solution and filled with 0.25% trypsin (Invitrogen/Gibco, Karlsruhe, Germany) for 30 minutes at 37°C. The trypsin was carefully aspirated and replaced with Dulbecco's modified Eagle's medium (DMEM; Biochrom, Berlin, Germany) supplemented with 10% fetal calf serum (FCS; Biochrom). The medium was gently agitated with a pipette, releasing the RPE into the medium by avoiding damage to Bruch's membrane. The suspended RPE cells were then transferred to a 35-mm^2 Petri dish and checked by microscope for cross contamination.

Human RPE Cell Culture

The RPE cell suspension was transferred to a 50-mL flask (Falcon, Wiesbaden, Germany) containing 20 mL of DMEM (Biochrom) supplemented with 20% FCS (Biochrom) and maintained at 37°C and 5% CO_2. Epithelial origin was confirmed by immunohistochemical staining for cytokeratin (CK) using a pan-CK antibody (Sigma-Aldrich, Deisenhofen, Germany).[34] The cells were tested and found free of contaminating macrophages (anti-CD11; Sigma) and endothelial cells (anti-von Willebrand factor, Sigma-Aldrich; data not shown). After reaching confluence, primary RPE cells were subcultured to passages 2 to 3 and maintained in DMEM (Biochrom) supplemented with 10% FCS (Biochrom) at 37°C and 5% CO_2. Cells were grown on plastic 10-cm tissue culture dishes until they had reached no more than 80% to 90% confluence, to assure that they are still in a proliferative, presumably dedifferentiated, state, and were then maintained under serum-free conditions for 48 hours to reduce the influence of serum stimulation.

Sample Preparation

For preparation of protein lysates from native RPE cell preparations, suspensions of freshly isolated human RPE cells were transferred to a 2.0-mL microcentrifuge tube and washed twice in Ca^{2+}-Mg^{2+}–free 1× phosphate-buffered saline (PBS; pH 7.4), followed by centrifugation at 800 rpm for 5 minutes. Cell pellets were then resuspended in nanopure water containing a protease inhibitor cocktail (Complete Mini; Roche Diagnostics, Inc., Mannheim, Germany) and snap frozen in liquid nitrogen. Cells were then disrupted by grinding with a Teflon glass homogenizer (Braun Biotech International, Melsungen, Germany), lyophilized, and stored at −80°C for future use. Proteins were solubilized in denaturing lysis buffer containing 9 M urea (Merck, Darmstadt, Germany), 2 M thiourea (Merck), 4% 3-([3-cholamidopropyl]dimethylammonio-2-hydroxy-1-propanesulfonate (CHAPS; Sigma-Aldrich), 1% dithioerytherol (Merck), 2.5 μM EGTA (Sigma-Aldrich), 2.5 μM EDTA (Sigma-Aldrich), and protease inhibitors for 4 hours at room temperature (RT). To minimize interindividual differences in native human RPE, protein lysates from five age-matched donor eyes were pooled.

For isolation of whole cellular protein extracts from RPE cultures, cells were washed once with serum-free medium, followed by a wash in 1× PBS (pH 7.4) and a third wash in 0.5× PBS to reduce contamination with salts. Subsequently, cells were collected and lysed in denaturing lysis buffer, as described earlier. Lysates were then cleared by centrifugation at 22,000*g* for 45 minutes at RT. Protein concentrations were determined by the Bradford protein assay reagent (Bio-Rad, Munich, Germany). Freshly prepared lysate containing 125 μg total protein was loaded onto each gel.

Two-Dimensional Electrophoresis

First-dimension isoelectric focusing (IEF) was performed with precast 18-cm immobilized pH gradient (IPG) strips (18 cm Immobiline DryStrip 3-10 NL; Amersham Pharmacia Biotech, Braunschweig, Germany). IPG strips were rehydrated overnight with 125 μg protein diluted to 350 μL with reswelling solution (9 M urea, 2 M thiourea, 4% CHAPS, 2.5 μM EGTA, 2.5 μM EDTA, 1% DTE, 4 mM Tris, 0.25% (wt/vol) bromophenol blue (BPB), and 0.7% (vol/vol) IEF ampholytic carriers (Pharmalytes pH 3–10; Amersham Pharmacia Biotech). IEF was performed at 20°C with a commercial system (Multiphore II; Amersham Pharmacia Biotech), with the initial voltage limited to 50 V (2 hours) and then increased stepwise to 8000 V and held until 101 kV/h was reached. Immediately after IEF, the IPG strips were equilibrated for 10 minutes in buffer containing 6 M urea, 2% SDS, 50 mM Tris-HCl (pH 6.8), 30% glycerol, and a trace of BPB under reducing conditions (65 mM DTE added), followed by another 10-minute incubation in the same buffer under alkylating conditions (135 mM iodoacetamide added). Equilibrated IPG strips were then placed on top of 9% to 15% linear gradient polyacrylamide gels 20 cm × 18 cm × 0.75 mm in size and embedded in 0.5% agarose (Serva, Heidelberg, Germany) in running buffer (384 mM glycin, 50 mM Tris, 0.2% SDS) and electrophoresed at a constant current of 8 mA/gel at 10°C, until the dye front had reached the bottom of the gel (approximately 16 hours). All gels were silver stained[35] and dried between cellophane sheets.

Image Analysis

Of the 12 silver-stained gels per cell type (native RPE; dedifferentiated cultured RPE), the 3 best focusing results were selected for calculating a virtual average gel on computer (Z3 software package; Compugen, Haifa, Israel). The computational calculation of virtual average gels reduced spot variations in individual gels from one sample resulting from limitations in two-dimensional electrophoresis (2-DE) reproducibility. Because spot integration of more than three gels from a given sample resulted in reduced quality of the virtual average gel, no more than three 2-DE gels per cell type were included in the virtual average gel. To create the virtual average gel, silver-stained 2-DE gels were scanned at 12 bit/300 dpi. Scans were then matched for each of the two cell types, using 42 to 56 common spots as landmarks, and processed on computer (in the Z3 Raw Master Gel [RMG]mode; Compugen). Next, spot detection was performed on each RMG by image analysis software (PD-Quest; Bio-Rad). RMGs from a given experimental condition (differentiated native versus dedifferentiated cultured

RPE) were analyzed manually to determine quantitative and qualitative differences in protein expression, because computer-assisted software comparison failed to integrate the rather diverse protein patterns stemming from differentiated native versus dedifferentiated cultured RPE.

In-Gel Digestion and MALDI-TOF Analysis

Central areas (2 × 2 mm) of silver stained spots were excised from dried 2-DE gels, transferred to 96-well plates (Nunc 22-260; Nunc, Wiesbaden, Germany), rehydrated in 100 μL nanopure water for a minimum of 30 minutes, destained with 30 mM potassium ferricyanide (Sigma-Aldrich) and 100 mM sodium thiosulfate (Merck),[36] and washed three times in 100 μL 40% acetonitrile (15 minutes each) to extract residual water. Acetonitrile was then removed, and a 10-μL digestion solution containing 0.01 μg/μL trypsin (Sequencing Grade Modified Trypsin; Promega, Mannheim, Germany) in 1 mM Tris-HCl (pH 7.5) was added for enzymatic cleavage.

After incubation under humid conditions at 37°C for 12 hours, 0.5 μL aliquots of the tryptic digests were mixed with 0.5 μL matrix consisting of 2,5-dihydroxybenzoic acid (Sigma-Aldrich; 20 mg/mL in 20% acetonitrile and 0.1% trifluoroacetic acid [TFA]) and 2-hydroxy-5-methoxybenzoic acid (Fluka, Buchs, Switzerland; 20 mg/mL in 20% acetonitrile and 0.1% TFA) at a 9:1 ratio (vol/vol) and spotted onto a 400-μm anchor steel target (Bruker-Daltronik, Bremen, Germany). MALDI-TOF peptide mass fingerprints were obtained on a mass spectrometer (Reflex III; Bruker-Daltronik) equipped with an ion source. Mass analyses obtained in the positive ion reflector mode were run automatically. For calibration, angiotensin-2-acetate (M_r 1046.54), substance P (M_r 1347.74), bombesin (M_r 1619.82), and ACTH 18-3 (M_r 2465.20) were recorded. Internal calibration using peptides resulting from autodigestion of trypsin was also performed.

Database Research

Trypsin specifically cleaves proteins at the C terminus of lysine and arginine residues, thereby generating a fingerprint of peptide masses that can be searched in databases. Database searches were performed with the assistance of commercial software (Mascot software; Matrix Science, London, UK).[37] Parameter settings were 150 ppm mass accuracy with one miscleavage allowed, and the search was performed in all available mammalian and, in assorted cases, all eukaryotic sequences. Peptide mass fingerprints (PMFs) were searched for matches with the virtually generated tryptic protein masses of the protein databases NCBInr (http://ncbi.nih.gov/ National Center for Biotechnical Information, Bethesda, MD), MSDB (csc-fserve.hh.med.ic.ac.uk/msdb.html/ Proteonomics Department, Hammersmith Campus, Imperial College, London, UK), and EnsemblC (http://www.ensembl.org/ Sanger Centre, Hinxton, UK). A protein was regarded as identified, if the following four criteria were fulfilled: (1) the MOWSE score[38] (http:www.hgmp.mrc.ac.uk/ Molecular Weight Search, Human Genome Mapping Project Resource Centre, Sanger Centre) was above the 5% significance threshold for the respective database, (2) the matched peptide masses were abundant in the spectrum, (3) the theoretical isoelectric point (pI) and the molecular weight (M_r) of the search result could be correlated with the 2-DE position of the corresponding spot, and (4) the matched sequence did not contain more than 20% uncleaved peptides. Functional classification was based on the classification provided in the TrEMBL (http://embl-heidelberg.de/ European Molecular Biology Laboratory, Heidelberg, Germany) and SwissProt protein knowledge databases (http://www.expasy.org/ Swiss Institute of Bioinformatics, Geneva, Switzerland). All databases are provided in the public domain by the host institutions.

Results

2-DE and Image Analysis

It was the main objective of this study to identify those proteins that are differentially expressed as a result of RPE dedifferentiation in vitro. To probe this proteomic shift, 2-DE gels of differentiated native and dedifferentiated cultured human RPE cells were analyzed. Figures 1 and 2 show the computationally estimated average RMG images of differentiated native RPE cells (Fig. 1) and of dedifferentiated cultured RPE cells (Fig. 2). Spot identification by the image analysis software (PD-Quest; Bio-Rad) allowed for the resolution of 1985 to 2014 spots in the RMGs of both cell types. Although 2-DE gels from differentiated native and dedifferentiated cultured RPE cells exhibited certain identical protein expression profiles, the images were too different to apply a computational comparative image analysis. For this reason, RMGs were manually compared, and the most distinct differentially expressed proteins were chosen for protein identification. Furthermore, randomly selected high-abundance protein spots found in both cell types were excised to serve as landmark proteins.

Protein Identification

Proteins were identified from 71 of 88 gel spots excised from 2-DE gels of native RPE and from 62 of 91 gel spots cut from the cultured RPE cell samples, for an average spot identification yield of 74%. For 20% of the remainder, the MS data were of insufficient quality, and protein identification was not possible. Another 3.1% could not be identified because of contamination of the tryptic digests with keratins, and no identity could be assigned to a further 2.9% despite good MS data, most likely because there was none of the respective sequences in the databases used.

Identified proteins, accession numbers, and SwissProt entry names are listed in Tables 1 and 2. Theoretical M_r, pI, percentage of sequence coverage, probability based MOWSE score, and functional category are also included. In addition, the spot numbers are assigned on the individual RMG images in Figures 1 and 2.

As seen before from 2-DE analysis, 25 proteins of a total of 90 different proteins identified were found in multiple spots on several positions on the gel. For example, two spots were found at the same M_r but separated by approximately 0.5 pH units (N62,N63 cathepsin D; N31,N35 F1-ATPase-β chain), and one protein was found at different M_rs but with the same pI (C4,C18; glucosidase II). Finally, four proteins were identified at slightly different M_rs and pIs (N58,N61 CRALBP; N5,N7 mitofilin; C45,C46 14-3-3 protein; C41,C42,C43 tropomyosin alpha, tropomyosin 4, tropomyosin alpha 3 chain.), suggesting the presence of different isoforms. These patterns clearly differed from a more frequently observed configuration, where spots were aligned like strings of pearls. This was observed for 15 proteins, which are represented with a series of two to three different spots, close together in a row (e.g., N14,N15,N19 annexin VI; N27,N28 S-arrestin; N22,N23 RPE65; C29,C30 α-enolase; C32,C33 CK 18). Such a series of spots is probably due to glutamine deamidation, chemically induced during the 2-DE procedure and resulting in differentially charged proteins rather than different protein isoforms.[39] We also mapped one protein (N1 cathepsin D) at a position on the gel that indicated a greater M_r than predicted and another two spots (C11 LIM-motif containing protein kinase; C31 eIF-4A_I) appeared at a pI different from the predicted one. In addition, retinal pigment epithelial membrane receptor (N34) was annotated at a position that differed in M_r and pI from the predicted values. Computer assisted sequence analysis identified this protein as a bovine isoform of RPE65, in this case, probably representing a partially processed stable fragment with different M_r and pI.

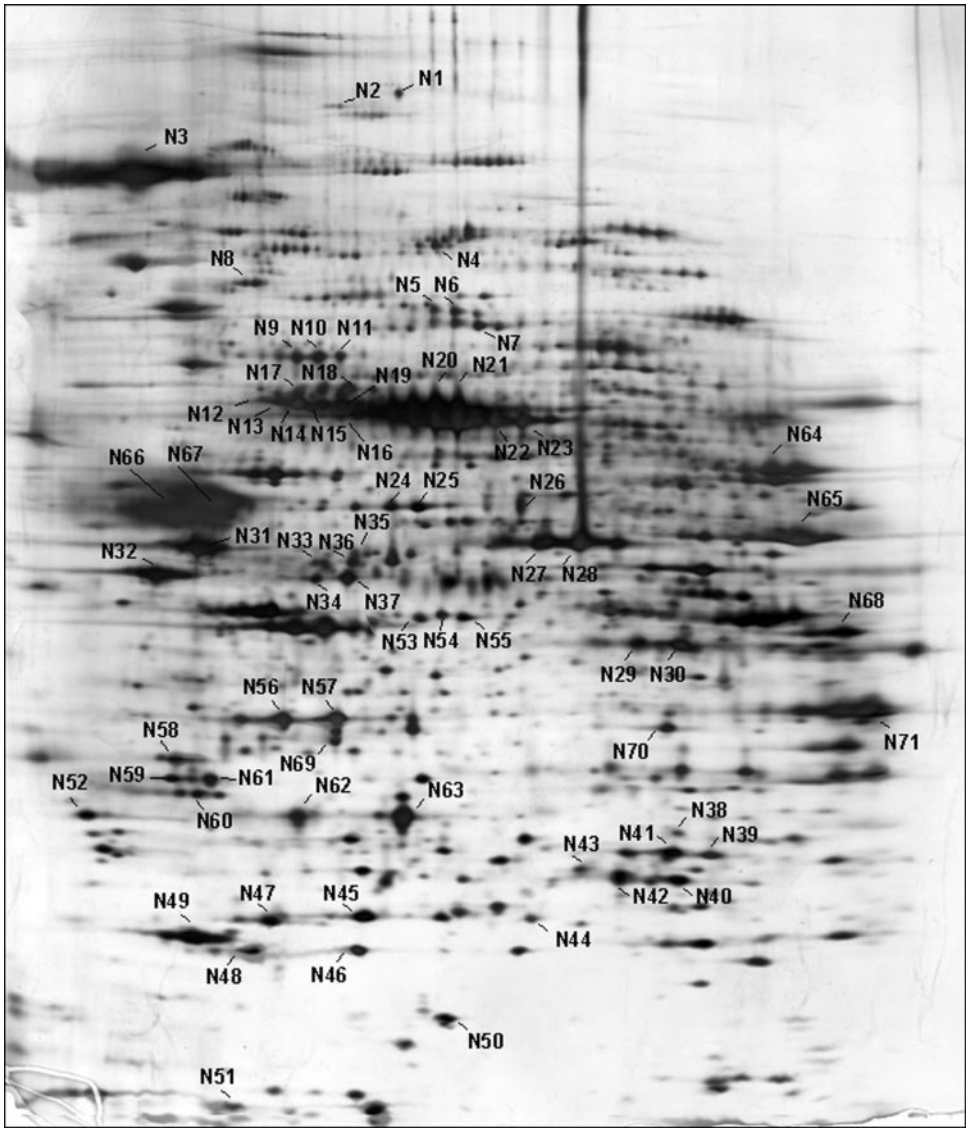

FIGURE 1. Silver-stained 2-DE image of differentiated native human RPE cells. Differentiated native human RPE cells were freshly isolated from human donor eyes and processed as described in Materials and Methods. Approximately 125 μg of protein was separated on an 18-cm, pH 3 to 10 nonlinear IPG strip, followed by 9% to 15% SDS-PAGE. The images are virtual average images calculated from three real gel images. Numbered *spots* were identified by MALDI-TOF MS and are listed in Table 1.

Comparison of the Differentiated Native RPE Proteome with That of Dedifferentiated Cultured RPE Cells

Overall the proteome of native and cultured RPE cells displayed a high degree of similarity, but at the same time striking distinguishing marks were apparent. Proteins were defined as differentially expressed if they could not be located to the corresponding position on the 2-DE gel of the other cell type. Expression below or above the detection limit of 2-DE technology was referred to as down- or upregulation of the respective proteins.

Expression Unchanged

In a first step, randomly selected high-abundance proteins that were located in identical positions and expression levels on gels of both groups were excised to serve as landmark proteins (Tables 1 and 2). Most of these proteins were found to be involved in metabolism (e.g., N71,C35 GADPH; N40,C55 triosephosphate isomerase). A high degree of similarity was also observed for molecular chaperones (e.g., N12,C12 heat shock 71 kDa protein) and antioxidant enzymes (e.g., N45,C49 glutathione S-transferase; N56,C50 peroxiredoxin 2). Good matching was found for the Ca^{2+}-binding proteins annexin V (N59,C44) and annexin VI (N19,C8) and for several proteins involved in signal transduction (e.g., N56,C38; GTP-binding regulatory protein; N52,C45 14-3-3 protein epsilon). A good correlation between differentiated native and dedifferentiated cultured RPE was also observed regarding f1-ATPase (N31) and ATP synthase (N48), two mitochondrial enzymes contributing to oxidative phosphorylation, as well as for CK 8 (N53,C24), an intermediate filament protein characteristic of cells of epithelial origin. Furthermore, the lysosomal enzyme cathepsin D (N62,N63,C58) was identified in both cell types, although it appeared to be expressed at a lower level in dedifferentiated, cultured RPE.

Proteins Downregulated or Absent in Dedifferentiated Cultured RPE

Although most of the metabolic enzymes identified could be found in both, differentiated and dedifferentiated RPE, a considerable group of metabolic enzymes expressed in the native RPE proteome could not be located in the corresponding positions on 2-DE gels of dedifferentiated RPE (Table 3). These included functions in glycolysis (N29 fructose-bisphosphate aldolase; N32 neuronal gamma enolase), in the tricarboxylic acid cycle (N54 succinyl-CoA ligase), and in protein metabo-

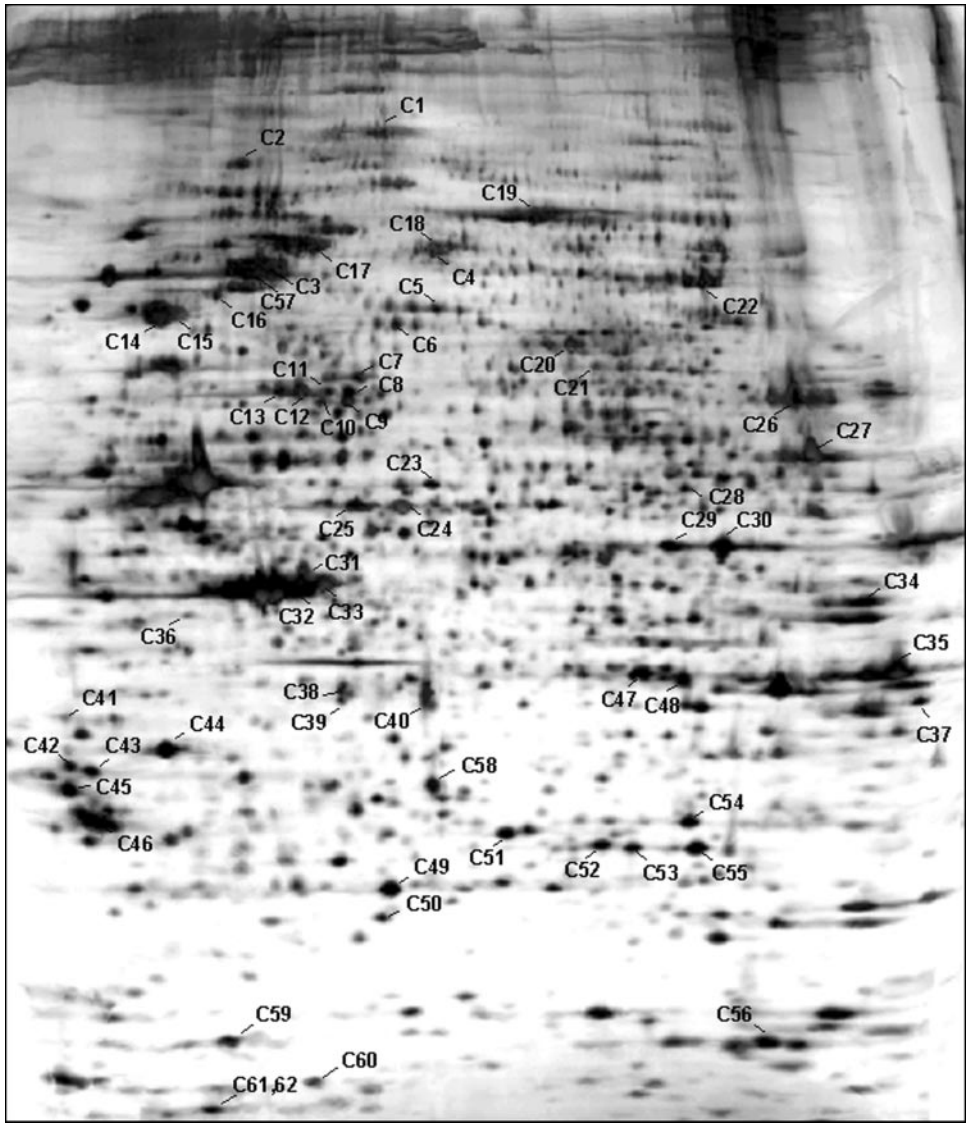

FIGURE 2. Silver-stained 2-DE image of dedifferentiated cultured primary human RPE cells of passage 3. RPE cells were grown on tissue culture plastic plates until they reached 80% to 90% confluence. Cells were then depleted of serum for 48 hours and harvested. Processing was as in Figure 1. Numbered *spots* are identified in Table 2.

lism (N26; prenylcysteine lyase). High-abundance proteins exclusively identified in differentiated RPE included interphotoreceptor retinoid-binding protein (N3; IRBP), an all-*trans* retinol and 11-*cis* retinal-binding protein located in the interphotoreceptor matrix, cellular retinol-binding protein (N51, CRBP), RPE65 (N22,N23) and cellular retinaldehyde-binding protein (N58,N61; CRALBP), all of which are involved in retinoid metabolism. Furthermore, we could not map the visual cycle proteins cone arrestin (N33,N36), S-arrestin (N27,N28), recoverin (N49), and phosducin (N60), as well as the mitochondrial motor protein mitofilin (N5,N6,N7) in 2-DE gels of cultured RPE. A significant difference was also observed in expression levels of mitochondrial proteins involved in electron transfer (N9,N10,N11 NADH-ubiquinone oxidoreductase; N37 ubiquinol-cytochrome-c reductase core protein I).

Proteins Upregulated in Dedifferentiated Cultured RPE

Marked upregulation in dedifferentiated RPE was found for proteins involved in cell shape, adhesion, exocytosis, and cytoskeleton formation. A summary of proteins upregulated in dedifferentiated RPE is provided in Table 4. Specific functions are also included.

These include the F-actin binding proteins α-actinin-1 (C3) and -4 (C57), which anchor F-actin to a variety of intracellular structures, as well as coactosin (C60). Further, an enhanced expression of vinculin (C19), a protein involved in cell adhesion, was observed. The expression of intermediate filament proteins was also altered. Both, differentiated and dedifferentiated RPE expressed CK 8 (N53,C24) and 18 (C32,C33), whereas dedifferentiated RPE cells also expressed CK-7 (C25) and -19 (C36). Furthermore, dedifferentiated cultured RPE cells expressed three isoforms of tropomyosin (C41, C42, and C43), a protein associated with stress fiber formation. Cultured cells also displayed a high abundance of ubiquitin-protein ligase (C17), annexin I (C47), annexin II (C48), translation initiation factor (eIF)-5A (C59), and eIF-4A_I (C31), which are expressed at lower levels or are missing in native RPE.

DISCUSSION

Proteomics refers to the study of the proteome—that is, the total protein complement of a genome. Unlike the genome, which is essentially the same in all somatic cells of an organism, the proteome is a dynamic entity that is not only different in different cell types, but also changes with the physiological

TABLE 1. Proteins Identified in Differentiated Native Human RPE Cells

Spot No.	SwissProt Entry Name	Accession No.	Protein Name	Organism	MOWSE Score	M_r (dalton)	Sequ. Cov. (%)	pI	Functional Category
N1	CATD_HUMAN	CATD_HUMAN	Cathepsin D (EC 3.4.23.5), chain B	Human	115	26457	44	5.31	Protein metabolism
N2	TRP_HUMAN	S33124	Tpr protein	Human	101	238770	10	5.05	Signal transduction
N3	IRBP_HUMAN	AAC18875	Interphotoreceptor retinoid-binding protein	Human	107	135603	27	4.79	Retinoid metabolism
N4	Q14697	Q14697	Glucosidase II Precursor	Human	101	107289	16	5.71	Glucose metabolism
N5	Q9P0V2	Q9P0V2	Mitofilin	Human	83	68316	15	5.71	Motor protein
N6	Q9P0V2	Q9P0V2	Mitofilin	Human	94	68316	24	5.57	Motor protein
N7	Q9P0V2	Q9P0V2	Mitofilin	Human	103	68316	22	5.57	Motor protein
N8	TERA_HUMAN	T02243	Probable transitional endoplasmic reticulum ATPase	Human	149	89950	31	5.14	Transport
N9	NUAM_HUMAN	AAH22368	NADH-ubiquinone oxidoreductase 75 kDa subunit	Human	148	80443	38	8.89	Energy metabolism
N10	NUAM_HUMAN	AAH22368	NADH-ubiquinone oxidoreductase 75 kDa subunit	Human	122	80443	27	5.89	Energy metabolism
N11	NUAM_HUMAN	AAH22368	NADH-ubiquinone oxidoreductase 75 kDa subunit	Human	106	80443	33	5.89	Energy metabolism
N12	HS7C_CRIGR	HS7C_CRIGR	Heat shock cognate 71 KD protein	*Cricetelus griseus*	109	70989	45	5.24	Chaperone
N13	HS7C_HUMAN	HS7C_HUMAN	Hsc70; Hsp73: dnaK-type molecular chaperone	Human	233	71082	40	5.37	Chaperone
N14	ANX6_HUMAN	ANX6_HUMAN	Annexin VI	Human	197	76037	38	5.42	Unclassified
N15	ANX6_HUMAN	ANX6_HUMAN	Annexin VI	Human	121	76037	28	5.42	Unclassified
N16	GR75_CRIGR	AAB62091	70kDa heat shock protein precursor, (75kDA glucose regulated protein)	*Cricetelus griseus*	196	73970	47	5.87	Chaperone
N17	GR75_HUMAN	B48127	70kDa heat shock protein precursor, (75kDA glucose regulated protein)	Human	111	73920	30	5.87	Chaperone
N18	GR75_HUMAN	B48127	70kDa heat shock protein precursor, (75kDA glucose regulated protein)	Human	148	73920	35	5.87	Chaperone
N19	ANX6_HUMAN	ANX6_HUMAN	Annexin VI	Human	324	76037	57	5.42	Unclassified
N20	ALBU_HUMAN	CAA01217	Mature human serum albumin (fragment)	Human	288	68425	50	5.67	Unclassified
N21	ALBU_HUMAN	CAA01217	Mature human serum albumin (fragment)	Human	328	68425	62	5.67	Unclassified
N22	Q16518	Q16518	Retinal pigment epithelium-specific 61 kDa protein	Human	94	61650	23	6.04	Retinoid metabolism
N23	Q16518	Q16518	Retinal pigment epithelium-specific 61 kDa protein	Human	151	61650	28	6.02	Retinoid metabolism
N24	PDA3_HUMAN	S55507	Protein disulfide-isomerase (EC 5.3.4.1) precursor	Human	151	57043	43	6.1	Protein metabolism
N25	PDA3_HUMAN	JC5704	Protein disulfide-isomerase (EC 5.3.4.1) precursor	Human	106	57012	23	5.93	Protein metabolism
N26	PCLI_HUMAN	AAF16937	Homo sapiens prenylcysteine lyase (PCLI)	Human	94	57012	41	5.81	Protein metabolism
N27	ARRS_HUMAN	AAC50992	Human arrestin (SAG)	Human	164	45234	49	6.14	Visual transduction cascade
N28	ARRS_HUMAN	AAC50992	Human arrestin (SAG)	Human	201	45234	49	6.14	Visual transduction cascade
N29	ALFC_HUMAN	ALFC_HUMAN	Fructose-bisphosphate aldolase C (EC 4.1.2.13) (Brain-type aldolase)	Human	142	39699	40	6.42	Glucose metabolism
N30	ALFC_HUMAN	ALFC_HUMAN	Fructose-bisphosphate aldolase C (EC 4.1.2.13) (Brain-type aldolase)	Human	144	39699	39	6.42	Glucose metabolism
N31	ATPB_RAT	IMABB	F1-ATPase beta chain beta chain (EC 3.6.1.34), chain B	Rat	152	49043	41	5.11	Energy metabolism
N32	ENOG_HUMAN	NOHUG	Phosphopyruvate hydratase (EC 4.2.1.11) gamma; gamma enolase; neuronale enolase	Human	121	47581	32	4.91	Glucose metabolism
N33	ARRC_HUMAN	ARRC_HUMAN	Cone arrestin	Human	104	43193	31	5.53	Visual transduction cascade
N34	Q05661	Q05661	Retinal pigment epithelial membrane receptor P63	Bovine	108	61616	33	6.0	Retinoid metabolism

(*continues*)

TABLE 1 (*continued*). Proteins Identified in Differentiated Native Human RPE Cells

Spot No.	SwissProt Entry Name	Accession No.	Protein Name	Organism	MOWSE Score	M_r (dalton)	Sequ. Cov. (%)	pI	Functional Category
N35	ATPB_RAT	IMABB	F1-atpase beta chain beta chain (EC 3.6.1.34), chain B	Rat	133	49043	45	5.11	Energy metabolism
N36	ARRC_HUMAN	ARRC_HUMAN	Cone arrestin	Human	94	43193	38	5.53	Visual transduction cascade
N37	UCR1_HUMAN	UCR1_HUMAN	Ubiquinol-cytochrome-c reductase (EC 1.10.2.2) core protein I	Human	113	53279	39	5.94	Energy metabolism
N38	CAHU1_HUMAN	CRHU1	Carbonate dehydrase (EC 4.2.1.1)I	Human	117	28909	41	6.59	Unclassified
N39	PMG1_HUMAN	PMG1_HUMAN	Phosphoglycerate mutase (EC 5.4.2.1) B chain	Rat	78	28928	56	6.67	Glucose metabolism
N40	TPIS_HUMAN	TPIS_HUMAN	Triosephosphate isomerase (EC 5.3.1.1)	Human	122	26807	54	6.51	Glucose metabolism
N41	PMG1_HUMAN	PMHUYB	Phosphoglycerate mutase (EC 5.4.2.1) B	Human	51	28900	22	6.67	Glucose metabolism
N42	TPIS_HUMAN	TPIS_HUMAN	Triosephosphate isomerase (EC 5.3.1.1)	Human	91	26807	46	6.51	Glucose metabolism
N43	AOP2_HUMAN	AOP2_HUMAN	Antioxidant protein 2 (1-Cys peroxiredoxin)	Human	131	25002	51	6.02	Antioxidant protein
N44	Q99497	JC5394	DJ-1 protein	Human	73	20063	43	6.33	Signal transduction
N45	GTP_HUMAN	CAA30894	Gluthatione S-transferase: (pi-family)	Human	133	23595	63	5.43	Antioxidant protein
N46	PDX2_HUMAN	PDX2_HUMAN	Peroxiredoxin 2 (thioredoxin peroxidase 1)	Human	99	22049	37	5.66	Antioxidant protein
N47	APA1_HUMAN	CAA00975	Apolipoprotein A1 precursor	Human	112	28061	39	5.27	Unclassified
N48	ATPQ_HUMAN	075947	ATP synthase D chain, mitochondrial (EC 3.6.1.34)	Human	119	18405	60	5.22	Energy metabolism
N49	RECO_HUMAN	RECO_HUMAN	Recoverin (cancer associated retinopathy protein) (CAR protein)	Human	155	23099	47	5.06	Visual transduction cascade
N50	NDKA_HUMAN	NDKA_HUMAN	Nucleoside diphosphate kinase A (EC 2.7.4.6)	Human	93	17309	47	5.88	Unclassified
N51	RETI_HUMAN	P09455	Cellular retinol-binding protein (CRBP)	Human	110	14382	61	4.74	Retinoid metabolism
N52	143E_HUMAN	S31975	14-3-3 protein epsilon, renal	Mouse	125	29326	44	4.63	Signal transduction
N53	K2C8_HUMAN	K2C8_HUMAN	Keratin, type II cytoskeletal 8 (cytokeratin 8)	Human	144	53510	33	5.52	Intermediate filament
N54	SCB1_HUMAN	Q9NVP7	Succinyl-CoA ligase (ADP-forming) beta-chain, mitochondrial	Human	121	48338	27	6.63	Tricarboxylic acid cycle
N55	Q9P129	Q9P129	Calcium-binding transporter	Human	98	46075	29	5.31	Unclassified
N56	GBB1_HUMAN	RGHUB1	GTP_binding regulatory protein beta-1 chain	Human	91	38020	25	5.6	Signal transduction
N57	GBB1_HUMAN	RGHUB1	GTP-binding regulatory protein beta-1 chain	Human	83	38020	25	5.6	Signal transduction
N58	CRAL_HUMAN	CRAL_HUMAN	Cellular retinaldehye-binding protein (CRALBP)	Human	142	36679	51	4.98	Retinoid metabolism
N59	ANX5_HUMAN	ANX5_HUMAN	Annexin V	Human	225	35840	62	4.94	Unclassified
N60	PHOS_HUMAN	A35422	Phosducin, retinal	Human	88	28513	27	5.08	Signal transduction
N61	CRAL_HUMAN	CRAL_HUMAN	Cellular retinaldehye-binding protein (CRALBP)	Human	122	36548	44	4.98	Retinoid metabolism
N62	CATD_HUMAN	ILYWB	Cathepsin D, chain B	Human	149	26457	65	7.5	Protein metabolism
N63	CATD_HUMAN	ILYWB	Cathepsin D, chain B	Human	155	26457	65	7.5	Protein metabolism
N64	KPY1_HUMAN	KPY1_HUMAN	Pyruvate kinase, M1 isozyme (EC 2.7.1.40)	Human	158	58280	31	7.57	Glucose metabolism
N65	ATPA_HUMAN	PWHUA	H+-transporting two-sector ATPase (EC 3.6.3.14) alpha chain precursor	Human	171	59828	34	9.16	Energy metabolism
N66	TBBX_HUMAN	Q8WUC	Tubulin beta 5	Human	117	50096	25	4.75	Cytoskeleton
N67	TBA1_HUMAN	177403	Tubulin alpha 1 chain	Human	103	50804	33	4.94	Cytoskeleton
N68	PGK1_HUMAN	KIHUG	Phosphoglycerate kinase (EC 2.7.2.3)	Human	129	44985	37	8.3	Glucose metabolism
N69	LDHH_HUMAN	LDHH_HUMAN	L-Lactate dehydrogenase H chain (EC 1.1.1.27), LDH-B	Human	74	36769	19	5.72	Glucose metabolism
N70	MDHC_HUMAN	MDHC_HUMAN	Malate dehydrogenase (EC 1.1.1.37)	Human	84	36500	27	6.89	Unclassified
N71	G3P2_HUMAN	G3P2_HUMAN	Glyceraldehyde 3-phosphate dehydrogenase (EC 1.2.1.12)	Human	121	36070	40	8.58	Glucose metabolism

Spot numbers are indicated in Figure 1. Accession numbers, protein name, and species identified are as listed in NCBInr, MSDB, and EnsemblC databases. Functional classification is based on TrEMBL and SwissProt classification.

TABLE 2. Proteins Identified in Dedifferentiated Cultured Human RPE Cells

Spot No.	SwissProt Entry Name	Accession No.	Protein Name	Organism	MOWSE Score	M_r (dalton)	Sequ. Cov. (%)	pI	Functional Category
C1	CLHI_HUMAN	CLHI_HUMAN	Clathrin heavy chain 1 (CLH-17)	Human	99	193260	21	5.48	Transport
C2	OXRP_HUMAN	OXRP_HUMAN	Oxygen-regulated protein 150K precursor	Human	92	111494	21	5.16	Chaperone
C3	AAC1_HUMAN	AAC1_HUMAN	Alpha-actinin 1, cytoskeletal isoform	Human	127	103480	27	5.22	Cytoskeleton
C4	Q14697	HSGLUCOII	Glucosidase II	Human	169	107289	25	5.71	Glucose metabolism
C5	GELS_HUMAN	GELS_HUMAN	Gelsolin precursor, plasma	Human	90	86043	17	5.9	Cytoskeleton
C6	KU86_HUMAN	KU86_HUMAN	ATP-dependent DNA helicase II, 86 kDa subunit	Human	80	83091	15	5.55	DNA-binding
C7	GR75_CRIGR	GR75_CRIGR	Mitochondrial stress-70 protein precursor (75 kDa glucose regulated)	*Cricetelus griseus*	204	73970	42	5.87	Chaperone
C8	ANX6_HUMAN	ANX6_HUMAN	Annexin VI (lipocortin VI)	Human	243	76168	37	5.42	Unclassified
C9	HS71_HUMAN	A45871	DnaK-type molecular chaperone HSP70-1	Human	171	70294	28	5.48	Chaperone
C10	HS71_HUMAN	A45871	DnaK-type molecular chaperone	Human	152	70294	26	5.48	Chaperone
C11	O54776	AB005132	LIM motif-containing protein kinase (EC 2.7.1.-)2	Mouse	82	71305	13	7.21	Signal transduction
C12	HS7C_HUMAN	A27077	Heat shock cognate 71 kDa protein	Human	153	71082	28	5.37	Chaperone
C13	HS7C_HUMAN	A27077	Heat shock cognate 71 kDa protein	Human	159	71082	30	5.37	Chaperone
C14	HS9A_HUMAN	HS9A_HUMAN	Heat shock protein HSP 90-alpha (HSP 86)	Human	125	84889	29	4.94	Chaperone
C15	HS9B_HUMAN	HS9B_HUMAN	Heat shock protein HSP 90-beta	Human	64	83554	13	4.97	Chaperone
C16	Q96112	Q96112	Proteasome (macropain) 26S subunit, non-ATPase	Human	108	100926	19	5.08	Protein metabolism
C17	UBC1_HUMAN	A38564	Ubiquitin-protein ligase (EC 6.3.2.19)	Human	90	118858	16	5.49	Protein metabolism
C18	Q14697	Q14697	Glucosidase II Precursor (KIAA0088 protein)	Human	144	107289	18	5.71	Glucose metabolism
C19	VINC_HUMAN	VINC_HUMAN	Vinculin (metavinculin)	Human	87	117088	18	5.83	Cell Adhesion
C20	Q96CU8	Q96CU8	Similar to villin 2 (ezrin)	Human	83	69484	14	5.94	Membrane-organization
C21	035763	AAB61666	Moesin	Rat	92	67868	17	6.16	Membrane-organization
C22	EF2_HUMAN	EF2_HUMAN	Elongation factor 2 (EF-2)	Human	102	96115	19	6.42	Protein metabolism
C23	PDA3_HUMAN	JC5704	Protein disulfide-isomerase (EC 5.3.4.1) precursor	Human	161	57043	35	5.98	Protein metabolism
C24	K2C8_HUMAN	K2C8_HUMAN	Keratin, type II cytoskeletal 8 (cytokeratin 8)	Human	266	53520	47	5.42	Intermediate filament
C25	K2C7_HUMAN	Q9BUD8	Keratin, type II cytoskeletal 7 (cytokeratin 7)	Human	209	51444	40	5.42	Intermediate filament
C26	TKT_HUMAN	A45050	Transketolase (EC 2.2.1.1)	Human	85	68435	24	7.9	Glucose metabolism
C27	KPY1_HUMAN	KPY1_HUMAN	Pyruvate kinase, M1 isozyme (EC 2.7.1.40)	Human	112	58280	29	7.57	Glucose metabolism
C28	ANXB_HUMAN	P50995	Annexin XI (56 kD autoantigen)	Human	90	54697	21	7.53	Unclassified
C29	ENOA_HUMAN	ENOA_HUMAN	Alpha enolase (EC 4.2.1.11) (non-neuronal enolase)	Human	175	47481	43	6.99	Glucose metabolism

(*continues*)

TABLE 2 (*continued*). Proteins Identified in Dedifferentiated Cultured Human RPE Cells

Spot No.	SwissProt Entry Name	Accession No.	Protein Name	Organism	MOWSE Score	M_r (dalton)	Sequ. Cov. (%)	pI	Functional Category
C30	ENOA_HUMAN	ENOA_HUMAN	Alpha enolase (EC 4.2.1.11); Non-neuronal enolase	Human	198	47350	56	6.99	Glucose metabolism
C31	IF41_HUMAN	CAA26843	Translation intiation factor eIF-4AI	Mouse	90	42386	29	6.56	Protein metabolism
C32	KICR_HUMAN	CAA31377	Keratin, type I cytoskeletal 18	Human	184	47305	36	5.27	Intermediate filament
C33	KICR_HUMAN	CAA31377	Keratin, type I cytoskeletal 18	Human	161	47305	37	5.27	Intermediate filament
C34	PGK1_HUMAN	KIHUG	Phosphoglycerate kinase (EC 2.7.2.3)	Human	101	44985	24	8.3	Glucose metabolism
C35	G3P2_HUMAN	G3P2_HUMAN	Glyceraldehyde 3-phosphate dehydrogenase (EC 1.2.1.12)	Human	98	36070	29	8.58	Glucose metabolism
C36	K1C2_HUMAN	KRHU	Keratin, type I, cytoskeletal 19	Human	94	44064	23	5.04	Intermediate filament
C37	ROA2_HUMAN	ROA2_HUMAN	Heterogeneous ribonuclear particle protein B1	Human	101	36041	38	8.67	RNA synthesis/ degradation
C38	GBB1_HUMAN	RGHUB1	GTP-binding regulatory protein beta-1 chain	Human	86	38151	24	5.71	Signal transduction
C39	GBB2_HUMAN	RGHUB2	GTP-binding regulatory protein beta-2 chain	Human	83	38048	31	5.6	Signal transduction
C40	LDHH_HUMAN	DEHULH	L-Lactate dehydrogenase H chain (LDH-B) (EC 1.1.1.27)	Human	87	36769	39	5.72	Glucose metabolism
C41	Q92XN6	AAK54243	Tropomyosin alpha isoform	Rat	104	33064	33	4.77	Cytoskeleton organization
C42	TPM4_HUMAN	CAA2888	Tropomyosin 4 type 2	Human	141	28522	40	4.77	Cytoskeleton organization
C43	TPM3_HUMAN	A25530	Tropomyosin alpha 3 chain	Human	189	29243	39	4.75	Cytoskeleton organization
C44	ANX5_HUMAN	ANX5_HUMAN	Annexin V	Human	171	35840	43	4.94	Unclassified
C45	143E_HUMAN	AAC37321	14-3-3 protein epsilon isoform	*Ovis aries*	129	26450	54	4.8	Signal transduction
C46	143Z_HUMAN	S65013	14-3-3 protein zeta chain	Cow	153	27810	60	4.73	Signal transduction
C47	ANX1_HUMAN	ANX1_HUMAN	Annexin I	Human	88	38787	28	6.64	Unclassified
C48	ANX2_HUMAN	ANX2_HUMAN	Annexin II	Human	189	38677	46	7.56	Unclassified
C49	GTP_HUMAN	CAA30894	Glutatione S-transferase (EC 2.5.1.18)	Human	81	23595	45	5.43	Antioxidant protein
C50	PDX2_HUMAN	CAA80269	Peroxiredoxin 2 (thioredoxin peroxidase 1)	Human	94	22104	28	6.84	Antioxidant protein
C51	HS27_HUMAN	E980237	HSP 27	Human	97	22427	38	7.83	Chaperone
C52	AOP2_HUMAN	AOP2_HUMAN	Antioxidant protein 2 (EC 1.11.1.7)	Human	87	25002	35	6.02	Antioxidant protein
C53	TPIS_HUMAN	TPIS_HUMAN	Triosephosphate isomerase (EC 5.3.1.1)	Human	64	26807	26	6.51	Glucose metabolism
C54	PMGI_HUMAN	PMHUYB	Phosphoglycerate mutase (EC 5.4.2.1) B	Human	94	28900	50	6.67	Glucose metabolism
C55	TPIS_HUMAN	TPIS_HUMAN	Triosephosphate isomerase (EC 5.3.1.1)	Human	116	26807	53	6.51	Glucose metabolism
C56	CYPH_HUMAN	CYPH_HUMAN	Peptidyl-prolyl cis-trans isomerase A (EC 5.2.1.8)	Human	93	18098	45	7.82	Protein metabolism
C57	AAC4_HUMAN	BAA24447	Alpha actinin 4	Human	271	102661	48	5.27	Cytoskeleton organization
C58	CATD_HUMAN	ILYWB	Cathepsin D (EC 3.4.23.5), chain B	Human	74	26457	31	5.31	Protein metabolism
C59	IF5A_HUMAN	IF5A_HUMAN	Initiation factor 5A (EIF-5A)(EIF-4D)	Human	75	16918	53	5.08	Protein metabolism
C60	Q14019	Q14019	CLP (fragment); Syn: Coactosin	Human	111	16049	54	5.54	Cytoskeleton organization

(*continues*)

TABLE 2 (*continued*). Proteins Identified in Dedifferentiated Cultured Human RPE Cells

Spot No.	SwissProt Entry Name	Accession No.	Protein Name	Organism	MOWSE Score	M_r (dalton)	Sequ. Cov. (%)	pI	Functional Category
C61	LEG1_HUMAN	LEG1_HUMAN	Galectin-1 (beta-galactoside-binding lectin L-14-1)	Human	88	14917	52	5.34	Unclassified
C62	THIO_HUMAN	JH568	Thioredoxin	Human	89	12015	59	4.82	Antioxidant

Spot numbers are indicated in Figure 2. Data sources are described in Table 1.

state of a cell. Ultimately, proteins expressed in dynamic compositions determine the phenotypic expression of genomic information. An important advantage of global protein expression profiling compared with individual gene regulation studies is the ability to monitor changes in several functional groups simultaneously. The objective of this study was to further elucidate differences in the protein expression profile of differentiated native compared with dedifferentiated cultured RPE cells and to use this information to clarify further the general understanding of ocular disease associated with RPE dedifferentiation. The data compiled in Tables 3 and 4 suggest that several biological processes were affected in the present study, and a few of these processes are discussed in this section.

Proteins Downregulated in Dedifferentiated Cultured Human RPE Cells

Phototransduction and Vitamin A Metabolism. In accordance with previous studies,[21,22,40,41] we observed a downregulation of proteins associated with retinoid metabolism (CRALBP, CRBP, RPE65, and IRBP) and the visual cycle (arrestin, recoverin) in dedifferentiated cultured RPE cells (for review, see Ref. 42). Whereas CRALBP, CRBP, and RPE65 are biochemical markers of RPE differentiation and rapidly become undetectable in culture,[21,40,41] identification of the latter ones in native RPE 2-DE gels may be due to photoreceptor cross-contamination of our RPE cell preparations. Despite extensive rinsing with PBS and repeated centrifugation at low speed, electron microscopy of consecutive sections revealed the presence of rod outer segment discs either in an intracellular location or bound to the RPE cell surface in our native RPE cell preparations (data not shown). The absence of IRBP, phosducin, brain-type fructose-bisphosphate aldolase, neuronal (gamma) enolase, and a retinal Ca^{2+}-binding transporter in 2-DE gels from dedifferentiated RPE further substantiate this consideration.

Energy Metabolism. Differentiated native RPE also exhibited a high abundance of the respiratory chain components

TABLE 3. Proteins Downregulated or Absent in Dedifferentiated Cultured Human RPE Cells

Spot No.	Protein Name	Function
N1, 62, 63	Cathepsin D (EC 3.4.23.5), chain B-human	Acid protease involved in intracellular protein breakdown
N2	Tpr protein	Involved in activation of oncogenic kinases
N3	Interphotoreceptor retinoid-binding protein	Shuttles retinoids between the retinol isomerase in the RPE and the visual pigments in the retina
N5-7	Mitofilin	Mitochandrial motor protein
N9-11	NADH-ubiquinone oxidoreductase 75 kDa subunit	Electron transfer/respiratory chain
N20, 21	Mature human serum albumin (fragment)	Serum component
N22, 23	Retinal pigment epithelium-specific 61 kDa protein	Involved in retinoid processing, presumed RPE membrane receptor for retinoids and component of isomerase system
N26	Homo sapiens prenylcysteine lyase (PCL1)	Involved in degradation of prenylated proteins
N27, 28	Human arrestin (SAG)	Binds photoactivated-phosphorylated rhodopsin, thereby arresting visual signal transduction
N29, 30	Fructose-bisphosphate aldolase C (EC 4.1.2.13)	Glycolysis; brain-type aldolase
N32	Phosphopyruvate hydratase (EC 4.2.1.11) gamma; neuronale enolase	Glycolysis; neuronal tissue-associated isoform
N33, 36	Cone arrestin	Presumably binds to photoactivated-phosphorylated red/green opsins
N34	Retinal pigment epithelial membrane receptor P63	Involved in retinoid processing, presumed RPE membrane receptor for retinoids
N35	F1-Atpase beta chain beta chain (EC 3.6.1.34), chain B	Respiratory chain
N37	Ubiquinolcytochrome-c reductase (EC 1.10.2.2) core protein 1	Electron transfer/respiratory chain
N47	Apolipoprotein A1 precursor	Participates in reverse transport of cholesterol from tissues to the liver
N49	Recoverin (cancer associated retinopathy protein) (CAR protein)	Neuronal Ca^{2+}-sensor protein: inhibition of the phosphorylation of rhodopsin in a Ca^{2+}-dependent manner; thought to prolong the light state
N51	Cellular retinol-binding protein 1 (CRBP)	Intracellular transport of retinol
N54	Succinyl-CoA ligase (ADP-forming) beta-chain	Involved in the tricarboxylic cycle: substrate level phosphorylation step
N55	Calcium-binding transporter, retinal	Ca^{2+}-dependent mitochondrial solute carrier
N58, 61	Cellular retinaldehyde-binding protein (CRALBP).	Retinoid metabolism: binds 11-*cis* retinal, involved in isomerization process
N60	Phosducin, retinal	GTP-binding protein: modulates phototransduction cascade by interacting with transducin

Spot numbers are indicated in Figure 1. Functional classification is derived from the TrEMBL and SwissProt databases (http://www.expasy.org).

TABLE 4. Proteins Upregulated in Dedifferentiated Cultured Human RPE Cells

Spot No.	Protein Name	Function
C1	Clathrin heavy chain 1 (CLH-17)	Major protein of the polyhedral coat of coated pits and vesicles
C2	Oxygen-regulated protein 150K precursor	Chaperone activity and cytoprotective role in cellular mechanisms triggered by oxygen deprivation
C3	Alpha-actinin 1, cytoskeletal isoform	Bundling protein: anchors actin to intracellular structures
C5	Gelsolin precursor	Actin-modulating protein: promotes assembly of actin monomers into filaments
C6	ATP-dependent DNA helicase II, 86 kDa subunit	Chromosome translocation, binds double-stranded DNA
C17	Ubiquitin protein ligase (EC 6.3.2.19)	Ubiquitination
C19	Vinculin (metavinculin)	Cell adhesion, involved in attachment of actin-based microfilaments to plasma membrane
C25	Keratin, type II cytoskeletal 7 (cytokeratin 7)	Intermediate filament protein
C31	Translation intiation factor eIF-4A_I	Initiation phase of protein synthesis
C36	Keratin, type I, cytoskeletal 19	Intermediate filament protein
C41	Tropomyosin alpha isoform	Stress fiber component; in nonmuscle cells implicated in stabilizing cytoskeleton actin filaments
C42	Tropomyosin 4	Stress fiber component; in nonmuscle cells implicated in stabilizing cytoskeleton actin filaments
C43	Tropomyosin alpha 3 chain	Stress fiber component; in nonmuscle cells implicated in stabilizing cytoskeleton actin filaments
C47	Annexin I	Membrane organization, exocytosis, control of cell growth
C48	Annexin II	Membrane organization, exocytosis, control of cell growth
C57	Alpha actinin 4	Actin binding protein; anchors actin to intracellular structures; colocalizes with actin stress fibers
C58	Initiation factor 5A (EIF-5A) (EIF-4D)	Initiation phase of protein synthesis
C60	CLP (fragment); Syn: Coactosin	Actin-binding protein, colocalizes with actin stress fibers
C61	Galectin-1 (beta-galactoside-binding lectin L-14-I)	Involved in regulation of cell differentiation, adhesion
C62	Thioredoxin	Participates in various redox reactions

Spot numbers are indicated in Figure 2. Functional classification source is provided in Table 3.

NADH-ubiqinone oxidoreductase and ubiqinol-cytochrome-c reductase,[43] both of which appeared to be downregulated in dedifferentiated cultured RPE cells. This may reflect the reduced energy requirement profile under cell culture conditions as opposed to the high-energy requirements in native RPE.[44]

Proteins Upregulated in Dedifferentiated Cultured Human RPE Cells

As expected, increased protein expression levels in dedifferentiated RPE cells can be attributed roughly to two functional groups: cytoskeleton remodeling and mediation of proliferative signal transduction.

Cell Shape, Migration, and Adhesion. Proteins associated with the keratin cytoskeleton, actin function, and maintenance of cell shape and motility appeared to be highly abundant in dedifferentiated cultured RPE cells. In agreement with previous studies we observed an altered expression of intermediate filament proteins in dedifferentiated cultured RPE cells.[23,45] CK 7, CK 8, CK 18, and CK 19 were highly abundant in dedifferentiated RPE, whereas cells isolated directly from the eye appeared to have no CK 7 and CK 19. CK 19 has been observed in proliferating RPE cells of patients with PVR[23] and has also been associated with migration in cultured human RPE cells.[45,46] In premalignant and malignant epithelial lesions,[47] CK 19 was correlated with infiltrating characteristics and invasive ability.

In addition to alterations in intermediate filament expression, we observed an increased expression of cytoskeleton-organizing proteins in dedifferentiated RPE cells. These included α-actinin, which can bundle actin filaments into parallel arrays[48]; gelsolin, an actin-binding protein that mediates rapid remodeling of actin filaments[49]; tropomyosins, which are a main component of stress fibers in mesenchymal cells; and coactosin, a recently identified human F-actin–binding protein that has also been co-localized with stress fibers.[50] In cultured fibroblasts α-actinin, gelsolin, and tropomyosin have been shown to be heavily enriched in stress fibers, which mediate cell contraction and migration.[49] Furthermore, dedifferentiated RPE cells displayed an upregulation of vinculin, a protein involved in cell adhesion.[51,52] Upregulation of these components may simply reflect a reorganization of the cellular cytoskeleton that is necessary for the cells to adopt to the new environment. Taken together, however, these changes may very well be coincidental with morphologic transformation and acquisition of migratory characteristics.

Cell Proliferation. A distinct observation from this study was the upregulation of proteins that can be attributed to cell proliferation. Annexins are a family of Ca^{2+}-dependent phospholipid-binding proteins that seem to be important regulatory proteins with pluripotent and pleiotropic roles. All annexins share the property of binding to acidic phospholipids of cellular membranes, suggesting a role in membrane-related events, particularly in membrane organization, exocytosis, and endocytosis.[53] We observed a strong upregulation of annexin I and II in dedifferentiated RPE cells, whereas annexin V and VI expression levels remained unchanged. In contrast to the latter ones, annexin I is a substrate of protein kinases involved in the control of cell growth and is postulated to be involved in mitogenic signal transduction.[54] Annexin II is also phosphorylated by tyrosin kinases and by protein kinase C.[55] Both annexin I and II are significantly overexpressed in various human cancers,[53,56,57] during liver regeneration and transformation,[58] and in proliferating cultured cells.[54]

Translation initiation factor (eIF)-4A_I and eIF-5A were expressed at detectable levels in dedifferentiated RPE cells exclusively. eIF-4A_I and eIF-5A belong to a group of proteins that control the initiation phase of eukaryotic protein synthesis. A series of observations suggest that these factors may also play major roles in the regulation of cell proliferation[59] and transformation (for review, see Ref. 60) Protein biosynthesis is one of the last steps in the transmission of genetic information on the basis of which proteins are produced to maintain the

specific biological function of a cell. Currently, an increasing body of data is emerging that shows that intervention in this pathway may be an additional target for antiproliferative strategies.[61,62]

Neither annexin I and II nor eIF-4A_I and eIF-5A have been described to play a role in RPE proliferation or dedifferentiation. Clearly, further studies are needed to evaluate the significance of these factors in control of RPE proliferation in vitro and in the situation found in PVR.

Conclusion

In the recent years, several studies have been attempted to analyze differential gene expression using cDNA-microarray technology. However, a cell's physiological state is ultimately dictated at the protein level, and comparison of cDNA expression levels to protein levels often reveals discrepancies between these two global expression approaches, demonstrating that transcript levels cannot predict protein levels.[63,64] Certainly, the inability to detect low-abundance proteins is a major drawback of the 2-DE technology. Despite this limitation, we were able to detect striking differences between differentiated and dedifferentiated RPE cells.

In the present study, we attempted to analyze dedifferentiated cultured RPE cells independent of ECM or serum stimulation in comparison with native differentiated RPE, and to draw conclusions about the potential role of RPE dedifferentiation in the onset of PVR. We are aware that the proper interpretation and clinical relevance of this study is limited by possible differences between cultured RPE cells and pseudometaplastic RPE cells in vivo, which are exposed to complex interactions that occur in the intraocular environment.

However, in summary, our data suggest a series of functional changes in dedifferentiated RPE cells in vitro, associated with the loss of RPE-specific functions, which add up to adaptive changes in cell phenotype toward a mesenchymal, migratory morphology, together with a high capacity to proliferate.

The results of this article focus attention onto a group of new proteins involved in cytoskeleton remodeling and cell proliferation, which may be involved in the initiation phase of PVR disease. Closer examination of these factors may lead to the definition of additional targets for treatment or prevention of ocular diseases associated with dedifferentiation and proliferation of RPE cells.

Acknowledgments

The authors thank Katja Obholzer for excellent technical assistance and Ursula Olazabal for a critical reading of the manuscript.

References

1. Grierson I, Hiscott P, Hogg P, Robey H, Mazure A, Larkin G. Development, repair and regeneration of the retinal pigment epithelium. *Eye.* 1994;8:255–262.
2. Zhao S, Rizzolo LJ, Barnstable CJ. Differentiation and transdifferentiation of the retinal pigment epithelium. *Int Rev Cytol.* 1997; 171:225–266.
3. Campochiaro PA, Hackett SF. Corneal endothelial cell matrix promotes expression of differentiated features of retinal pigmented epithelial cells: implication of laminin and basic fibroblast growth factor as active components. *Exp Eye Res.* 1993;57:539–547.
4. L'Esperance FA. The ocular histopathologic effect of krypton and argon laser radiation. *Am J Ophthalmol.* 1969;68:263–269.
5. Lincoff H, Kreissig I, Jakobiec F, Iwamoto T. Remodeling of the cryosurgical adhesion. *Arch Ophthalmol.* 1981;99:1845–1849.
6. Tso MO, Fine BS. Repair and late degeneration of the primate foveola after injury by argon laser. *Invest Ophthalmol Vis Sci.* 1979;18:447–461.
7. Korte GE, Perlman JI, Pollack A. Regeneration of mammalian retinal pigment epithelium. *Int Rev Cytol.* 1994;152:223–263.
8. Machemer R, van Horn D, Aaberg TM. Pigment epithelial proliferation in human retinal detachment with massive periretinal proliferation. *Am J Ophthalmol.* 1978;85:181–191.
9. Machemer R, Laqua H. Pigment epithelium proliferation in retinal detachment (massive periretinal proliferation). *Am J Ophthalmol.* 1975;80:1–23.
10. Mueller-Jensen K, Machemer R, Roobik A. Autotransplantation of retinal pigment epithelium in intravitreal diffusion chamber. *Am J Ophthalmol.* 1975;80:530–537.
11. Mandelcorn MS, Machemer R, Fineberg E, Hersch SB. Proliferation and metaplasia of intravitreal retinal pigment epithelium cell autotransplants. *Am J Ophthalmol.* 1975;80:227–237.
12. Kampik A, Kenyon KR, Michels RG, Green WR, de la Cruz ZC. Epiretinal and vitreous membranes: comparative study of 56 cases. *Arch Ophthalmol.* 1981;99:1445–1454.
13. Machemer R. Proliferative vitreoretinopathy (PVR): a personal account of its pathogenesis and treatment. *Invest Ophthalmol Vis Sci.* 1988;29:1771–1783.
14. Glaser BM, Lemor M. Pathobiology of proliferative vitreoretinopathy. In: Ryan SJ, ed. *Retina.* St. Louis: Mosby-Year Book Press; 1994:2249–2263.
15. Campochiaro PA. Pathogenic mechanisms in proliferative vitreoretinopathy. *Arch Ophthalmol.* 1997;115:237–241.
16. Hiscott P, Sheridan C, Magee RM, Grierson I. Matrix and the retinal pigment epithelium in proliferative retinal disease. *Prog Retinal Eye Res.* 1999;18:167–190.
17. Newsome DA, Rodrigues MM, Machemer R. Human massive periretinal proliferation: in vitro characteristics of cellular components. *Arch Ophthalmol.* 1981;99:873–880.
18. Glaser BM, Cardin A, Biscoe B. Proliferative vitreoretinopathy: the mechanism of development of vitreoretinal traction. *Ophthalmology.* 1987;94:327–332.
19. Radtke ND, Tano Y, Chandler D, Machemer R. Simulation of massive periretinal proliferation by autotransplantation of retinal pigment epithelial cells in rabbits. *Am J Ophthalmol.* 1981;91:76–87.
20. Campochiaro PA, Hackett SF, Conway BP. Retinoic acid promotes density-dependent growth arrest in human retinal pigment epithelial cells. *Invest Ophthalmol Vis Sci.* 1991;32:65–72.
21. Hamel CP, Tsilou E, Pfeffer BA, Hooks JJ, Detrick B, Redmond TM. Molecular cloning and expression of RPE65, a novel retinal pigment epithelium-specific microsomal protein that is post-transcriptionally regulated in vitro. *J Biol Chem.* 1993;268:15751–15757.
22. Neill JM, Thornquist SC, Raymond MC, Thompson JT, Barnstable CJ. RET-PE10: a 61 kD polypeptide epitope expressed late during vertebrate RPE maturation. *Invest Ophthalmol Vis Sci.* 1993;34: 453–462.
23. Hunt RC, Davis AA. Altered expression of keratin and vimentin in human retinal pigment epithelial cells in vivo and in vitro. *J Cell Physiol.* 1990;145:187–199.
24. Casaroli-Marano RP, Pagan R, Vilaro S. Epithelial-mesenchymal transition in proliferative vitreoretinopathy: intermediate filament protein expression in retinal pigment epithelial cells. *Invest Ophthalmol Vis Sci.* 1999;40:2062–2072.
25. Turksen K, Opas M, Aubin JE, Kalnins VI. Microtubules, microfilaments and adhesion patterns in differentiating chick retinal pigment epithelial (RPE) cells in vitro. *Exp Cell Res.* 1983;147:379–391.
26. Rizzolo LJ. The distribution of Na+, K(+)-ATPase in the retinal pigmented epithelium from chicken embryo is polarized in vivo but not in primary cell culture. *Exp Eye Res.* 1990;51:435–446.
27. Huotari V, Sormunen R, Lehto VP, Eskelinen S. The polarity of the membrane skeleton in retinal pigment epithelial cells of developing chicken embryos and in primary culture. *Differentiation.* 1995;58:205–215.
28. Grisanti S, Guidry C. Transdifferentiation of retinal pigment epithelial cells from epithelial to mesenchymal phenotype. *Invest Ophthalmol Vis Sci.* 1995;36:391–405.
29. Vinores SA, Derevjanik NL, Mahlow J, et al. Class III beta-tubulin in human retinal pigment epithelial cells in culture and in epiretinal membranes. *Exp Eye Res.* 1995;60:385–400.

30. Campochiaro PA, Jerdan JA, Glaser BM. Serum contains chemoattractants for human retinal pigment epithelial cells. *Arch Ophthalmol.* 1984;102:1830–1833.
31. Lee SC, Kwon OW, Seong GJ, Kim SH, Ahn JE, Kay ED. Epitheliomesenchymal transdifferentiation of cultured RPE cells. *Ophthalmic Res.* 2001;33:80–86.
32. Ando A, Ueda M, Uyama M, Masu Y, Ito S. Enhancement of dedifferentiation and myoid differentiation of retinal pigment epithelial cells by platelet derived growth factor. *Br J Ophthalmol.* 2000;84:1306–1311.
33. Alge CS, Priglinger SG, Neubauer AS, et al. Retinal pigment epithelium is protected against apoptosis by αB-crystallin. *Invest Ophthalmol Vis Sci.* 2002;43:3575–3582.
34. Leschey KH, Hackett SF, Singer JH, Campochiaro PA. Growth factor responsiveness of human retinal pigment epithelial cells. *Invest Ophthalmol Vis Sci.* 1990;31:839–346.
35. Blum H, Beier H, Gross HJ. Improved silver staining of plant proteins, RNA, and DNA in polyacrylamide gels. *Electrophoresis.* 1987;8:93–99.
36. Gharahdaghi F, Weinberg CR, Meagher DA, Imai BS, Mische SM. Mass spectrometric identification of proteins from silver-stained polyacrylamide gel: a method for the removal of silver ions to enhance sensitivity. *Electrophoresis.* 1999;20:601–605.
37. Pappin DJ. Peptide mass fingerprinting using MALDI-TOF mass spectrometry. *Methods Mol Biol.* 1997;64:165–173.
38. Perkins DN, Pappin DJ, Creasy DM, Cottrell JS. Probability-based protein identification by searching sequence databases using mass spectrometry data. *Electrophoresis.* 1999;20:3551–3567.
39. Schmid DG, von der Mulbe FD, Fleckenstein B, Weinschenk T, Jung G. Broadband detection electrospray ionization Fourier transform ion cyclotron resonance mass spectrometry to reveal enzymatically and chemically induced deamidation reactions within peptides. *Anal Chem.* 2001;73:6008–6013.
40. Nicoletti A, Wong DJ, Kawase K, et al. Molecular characterization of the human gene encoding an abundant 61 kDa protein specific to the retinal pigment epithelium. *Hum Mol Genet.* 1995;4:641–649.
41. Crabb JW, Goldflam S, Harris SE, Saari JC. Cloning of the cDNAs encoding the cellular retinaldehyde-binding protein from bovine and human retina and comparison of the protein structures. *J Biol Chem.* 1988;263:18688–18692.
42. McBee JK, Palczewski C, Baehr W, Pepperberg DR. Confronting Complexity: the interlink of phototransduction and retinoid metabolism in the vertebrate retina. *Prog Retinal Eye Res.* 2001;20:469–529.
43. Nohl H. Generation of superoxide radicals as byproduct of cellular respiration. *Ann Biol Clin* (*Paris*). 1994;52:199–204.
44. Cai J, Nelson KC, Wu M, Sternberg P Jr, Jones DP. Oxidative damage and protection of the RPE. *Prog Retinal Eye Res.* 2000;19:205–221.
45. Robey HL, Hiscott PS, Grierson I. Cytokeratins and retinal epithelial cell behaviour. *J Cell Sci.* 1992;102:329–340.
46. Fuchs U, Kivela T, Tarkkanen A. Cytoskeleton in normal and reactive human retinal pigment epithelial cells. *Invest Ophthalmol Vis Sci.* 1991;32:3178–3186.
47. Nagle RB, Brawer MK, Kittelson J, Clark V. Phenotypic relationships of prostatic intraepithelial neoplasia to invasive prostatic carcinoma. *Am J Pathol.* 1991;138:119–128.
48. Pollard TD, Cooper JA. Actin and actin-binding proteins: a critical evaluation of mechanisms and functions. *Annu Rev Biochem.* 1986;55:987–1035.
49. Arora PD, Janmey PA, McCulloch CA. A role for gelsolin in stress fiber-dependent cell contraction. *Exp Cell Res.* 1999;250:155–167.
50. Provost P, Doucet J, Stock A, Gerisch G, Samuelsson B, Radmark O. Coactosin-like protein, a human F-actin-binding protein: critical role of lysine-75. *Biochem J.* 2001;359:255–263.
51. Opas M, Turksen K, Kalnins VI. Adhesiveness and distribution of vinculin and spectrin in retinal pigmented epithelial cells during growth and differentiation in vitro. *Dev Biol.* 1985;107:269–280.
52. McKay BS, Irving PE, Skumatz CM, Burke JM. Cell-cell adhesion molecules and the development of an epithelial phenotype in cultured human retinal pigment epithelial cells. *Exp Eye Res.* 1997;65:661–671.
53. Della Gaspera B, Braut-Boucher F, Bomsel M, et al. Annexin expressions are temporally and spatially regulated during rat hepatocyte differentiation. *Dev Dyn.* 2001;222:206–217.
54. Schlaepfer DD, Haigler HT. Expression of annexins as a function of cellular growth state. *J Cell Biol.* 1990;111:229–238.
55. Huang KS, Wallner BP, Mattaliano RJ, et al. Two human 35 kd inhibitors of phospholipase A2 are related to substrates of pp60v-src and of the epidermal growth factor receptor/kinase. *Cell.* 1986;46:191–199.
56. Masaki T, Tokuda M, Ohnishi M, et al. Enhanced expression of the protein kinase substrate annexin in human hepatocellular carcinoma. *Hepatology.* 1996;24:72–81.
57. Wu W, Tang X, Hu W, Lotan R, Hong WK, Mao L. Identification and validation of metastasis-associated proteins in head and neck cancer cell lines by two-dimensional electrophoresis and mass spectrometry. *Clin Exp Metastasis.* 2002;19:319–326.
58. de Coupade C, Gillet R, Bennoun M, Briand P, Russo-Marie F, Solito E. Annexin 1 expression and phosphorylation are upregulated during liver regeneration and transformation in antithrombin III SV40 T large antigen transgenic mice. *Hepatology.* 2000;31:371–380.
59. Williams-Hill DM, Duncan RF, Nielsen PJ, Tahara SM. Differential expression of the murine eukaryotic translation initiation factor isogenes eiF4-A_I and eIF4-A_{II} is dependent upon cellular growth status. *Arch Biochem Biophys.* 1997;333:111–120.
60. Caraglia M, Budillon A, Vitale G, Lupoli G, Tagliaferri P, Abbruzzese A. Modulation of molecular mechanisms involved in protein synthesis machinery as a new tool for the control of cell proliferation. *Eur J Biochem.* 2000;267:3919–3936.
61. Caraglia M, Marra M, Giuberti G, et al. The role of eukaryotic initiation factor 5A in the control of cell proliferation and apoptosis. *Amino Acids.* 2001;20:91–104.
62. Nishimura K, Ohki Y, Fukuchi-Shimogori T, et al. Inhibition of cell growth through inactivation of eukaryotic translation initiation factor 5A (eIF5A) by deoxyspergualin. *Biochem J.* 2002;363:761–768.
63. Anderson L, Seilhamer J. A comparison of selected mRNA and protein abundances in human liver. *Electrophoresis.* 1997;18:533–537.
64. Gygi SP, Rochon Y, Franza BR, Aebersold R. Correlation between protein and mRNA abundance in yeast. *Mol Cell Biol.* 1999;19:1720–1730.